Polymer Chemistry

PAPER

View Article Online
View Journal | View Issue

CrossMark click for updates

Cite this: *Polym. Chem.*, 2015, **6**, 7464

Received 31st May 2015,
Accepted 31st August 2015

DOI: 10.1039/c5py00829h

www.rsc.org/polymers

High performance polymers and their PCBM hybrids for memory device application†

Hung-Ju Yen,‡§ Chih-Jung Chen,‡ Jia-Hao Wu and Guey-Sheng Liou*

Three series of high ON/OFF ratio (~10^9) memory devices were prepared from OHTPA-based high-performance polymers with various amounts of PCBM. The memory behaviors of these devices can be tuned in a wide range from insulator through DRAM, SRAM to WORM by the concentration of the electron-acceptor PCBM.

Introduction

Recently, the application of electroactive materials in optoelectronic devices such as photovoltaic,[1] light-emitting diodes,[2] thin film transistors,[3] memory,[4] and electrochromic devices[5] has attracted tremendous attention, due to their structural flexibility, low-cost, solution processability, large area fabrication, and three-dimensional stacking capability.[6] The emergent investigation for information storage in the form of high (ON) and low (OFF) current states instead of the amount of charge stored in silicon devices is to improve and/or enhance the superiority of higher data storage density, ease of miniaturization, tunable data retention time, faster speed, lower power consumption, and cost-effective processing for practical utilization.[7] Polymeric materials with electrical bistability resulting from different electronic structures corresponding to the applied electric field begin to stand out conspicuously and have predominance in scaling down from micro-scale to nano-scale for memory device applications. Thus, polymeric memory devices have been developed as a promising alternative to the conventional semiconductor-based memory devices.

In the original development of memory devices, polymers were used as matrices and polyelectrolytes.[8] In recent years, the design and synthesis of polymers with specific structures that can provide the desired electronic properties is a crucial milestone in the development of efficient polymeric memory devices. For the materials used in resistive type memory devices, electron donor–acceptor polymers are considered as suitable materials because charge transfer (CT) from the donor to acceptor moieties can give rise to a highly conductive state.[4a] A few precedents using donor–acceptor systems have been demonstrated and can be divided into conjugated polymers,[9] polymers with pendent donors or acceptor moieties,[4b] functional polyimides, and polymer nanocomposites.[10]

Among these categories, the polymer nanocomposites were extensively prepared for memory devices owing to their excellent thermal stability, mechanical properties, and fine-tuned memory characteristics. Initially, polymers were used as matrices for small molecules.[8] Afterwards, the electroactive nano-fillers such as carbon nanotubes[11] and graphene oxides[12] were blended into the "donor-containing polymer". In particular, [6,6]-phenyl-C61-butyric acid methyl ester (PCBM)-containing hybrid films were most widely used as the active layer in the memory application.[13]

In our previous study, we fabricated the memory devices by blending the PCBM as the acceptor with the donor-containing poly-4-methoxytriphenylamine (**P-TPA**).[13a] Triphenylamine (TPA) and its derivatives are well-known candidates as hole transport materials for organic optoelectronic devices due to their resulting stable radical cations, good hole-mobility, and high thermal stability.[14] However, the memory devices based on **P-TPA**:PCBM hybrids only exhibited dynamic random access memory (DRAM) and the write-once-read-many-times (WORM) properties even control the concentration of PCBM particularly, and the intermediate static random-access memory (SRAM) cannot be obtained yet.

In this contribution, we strive to fabricate the memory devices by blending the electron-acceptor PCBM with hydroxytriphenylamine (OHTPA)-containing high performance polymers (Fig. 1). Non-conjugate OHTPA-based polymers are not only advantageous in increasing the ON/OFF ratio due to their low OFF current but are also expected to have a strong inter-

Functional Polymeric Materials Laboratory, Institute of Polymer Science and Engineering, National Taiwan University, 1 Roosevelt Road, 4th Sec., Taipei 10617, Taiwan. Fax: +886-2-33665237; Tel: +886-2-33665070; E-mail: gsliou@ntu.edu.tw

†Electronic supplementary information (ESI) available: Experimental section. Table: inherent viscosity, molecular weights, solubility behavior, thermal, and electrochemical properties. Figure: NMR, TGA, DSC, absorption spectra, CV, and current–voltage (*I–V*) characteristics. See DOI: 10.1039/c5py00829h

‡These authors contributed equally to this work.

§Present address: Physical Chemistry and Applied Spectroscopy (C-PCS), Chemistry Division, Los Alamos National Laboratory, Los Alamos, New Mexico 87545, USA.

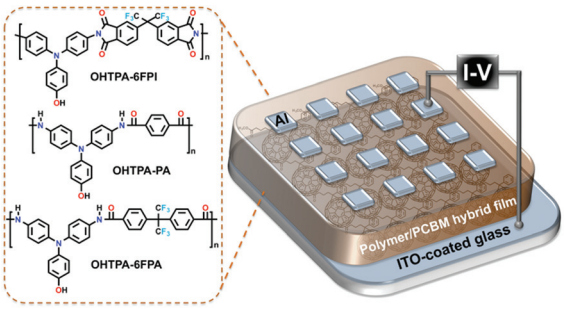

Fig. 1 Chemical structures of hybrid materials and configuration of the memory device.

action with PCBM, resulting in good dispersion and stable memory properties even at a high PCBM content.

Results and discussion

Synthesis and characterization

The preparation of the polyimide **OHTPA-6FPI** was carried out by a one-pot, high-temperature solution polycondensation method. In this procedure, dianhydride 4,4′-(hexafluoroisopropylidene)diphthalic anhydride and diamine **1** were polymerized in *m*-cresol at 210 °C in the presence of isoquinoline as the catalyst. On the other hand, polyamides **OHTPA-PA** and **OHTPA-6FPA** were synthesized by low-temperature polycondensation of diamine **1** with terephthaloyl chloride and hexafluoro-2,2-bis(4-chlorocarbonylphenyl)propane in the presence of propylene oxide as an acid acceptor, respectively (Scheme 1). Under these conditions, polymerization reactions proceeded homogeneously and led to the formation of highly viscous polymer solutions, then could be precipitated into the tough fiber-like form when slowly pouring the resulting polymer solutions into methanol. The inherent viscosities and molecular weight of these polymers are summarized in Table S1.† All these high molecular weight polymers could afford transparent and tough films *via* solution casting. NMR spectroscopic technique was used to identify the structures of the prepared polymers, where the spectra agree well with the proposed molecular structures (Fig. S1†).

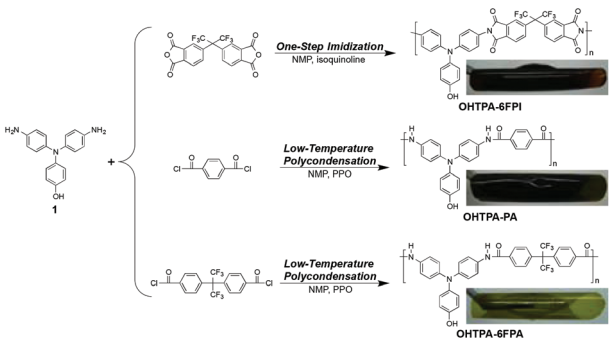

Scheme 1 Synthesis of OHTPA-based high-performance polymers.

Polymer properties

Solubility and film properties. The solubility behavior of these resulting polymers was investigated qualitatively, and the results are also listed in Table S2.† All the polymers were readily soluble in polar aprotic organic solvents such as NMP, *N*,*N*-dimethylacetamide (DMAc), *N*,*N*-dimethylformamide (DMF), and dimethyl sulfoxide (DMSO). Thus, the excellent solubility makes these polymers potential candidates for practical applications by spin-coating or inkjet-printing processes to afford high performance thin films for optoelectronic devices. As shown in Scheme 1, the polymers could be solution cast into flexible, transparent, and tough films. The high solubility can be attributed to the incorporation of a bulky and propeller-like nonplanar conformation OH-TPA moiety along the polymer backbone, which results in a high steric hindrance to prevent close packing, and thus reduces the crystallization tendency.

Thermal properties. The thermal properties of polymers were examined by TGA and DSC, and the thermal behavior data are summarized in Table S3.† TGA curves of these resulting polymers under both air and nitrogen atmospheres are shown in Fig. S2.† All the prepared polymers exhibited good thermal stability with insignificant weight loss up to 400 °C under a nitrogen or air atmosphere, and the carbonized residue (char yield) of these polymers under a nitrogen atmosphere was more than 59% at 800 °C. The glass-transition temperatures (T_g) could be easily measured in the DSC thermograms (as shown in Fig. S3†). In Table S3,† polyimide **OHTPA-6FPI** revealed a much higher T_g (324 °C) than the corresponding polyamide **OHTPA-6FPA** (314 °C), indicating polyimide **OHTPA-6FPI** with more chain stiffness as compared with the molecular structure of polyamide **OHTPA-6FPA**. In addition, these polymers revealed a remarkably increased T_g as a result of the presence of rigid TPA aromatic units.

Absorption and electrochemistry

The UV-vis absorption spectrum of polymers is depicted in Fig. S4† and the optical energy band gap (E_g) is estimated by the onset wavelength. The smaller band gap energy of polyimide **OHTPA-6FPI** (2.23 eV) as opposed to polyamides **OHTPA-PA** and **OHTPA-6FPA** (2.66 and 2.92 eV) is mainly due to the strong electron-deficient acceptor phthalimide unit, coupling with electron-rich TPA giving rise to a charge transfer characteristic accompanied by smaller band gap energy.

The electrochemical properties of polymers were investigated by cyclic voltammetry (CV) conducted by using a cast film on an indium-tin oxide (ITO)-coated glass slide as the working electrode in anhydrous acetonitrile, using 0.1 M tetrabutylammonium perchlorate as a supporting electrolyte under a nitrogen atmosphere. Typical CV diagrams for the polymers are shown in Fig. S5,† revealing one reversible oxidation redox couple at the onset potential (E_{onset}) of around 0.85 and 0.55 V for polyimide and polyamides, respectively. The redox poten-

tials of the polymers and their respective HOMO and LUMO are calculated and summarized in Table S4.†

Memory device characteristics

The resulting memory characteristics of **OHTPA-6FPI**, **OHTPA-PA**, **OHTPA-6FPA**, and their hybrid films were investigated by the current–voltage (*I–V*) characteristics of an ITO/polymer:PCBM/Al sandwich device. Within the sandwich device, the polymer film was used as an active layer between Al and ITO as the top and bottom electrodes, respectively (Fig. 1). The polymer film thickness was optimized around 50 nm and was used for all devices. Fig. 2 demonstrates the *I–V* result of **OHTPA-6FPI** and its hybrid films, which was measured with a compliance current of 0.01 A. Initially, the current of the as-fabricated device is low and no electrical switching capability is observed when scanning positively (the first sweep). During the second negative sweep from 0 V to −6 V, the device stayed in the OFF state with a current range at $\sim 10^{-12}$ A originally, followed by an abrupt increase to 10^{-3} A corresponding to the threshold voltage of −5.8 V, implying the transition from the OFF state to the ON state. In a memory device, this OFF-to-ON transition can be defined as a "writing" process. The device retained in the ON state during the subsequent negative scan (the third sweep) and then the positive scan (the fourth sweep), indicating the reading process. After turning off the power for about 30 seconds, the device could be re-programmed from the OFF state to the ON state again with the threshold voltage of −5.8 V (the fifth sweep). The ON state was found to relax to the OFF state without an erasing process but only removing the external applied bias. The short retention time of the ON state indicates that **OHTPA-6FPI** exhibits volatile DRAM memory behavior. This result differs from the work reported by Ree's group,[15] claiming that the hydroxyl groups both serve as an electron-donating group and provide one more possibility for charge trapping under an applied electric field.

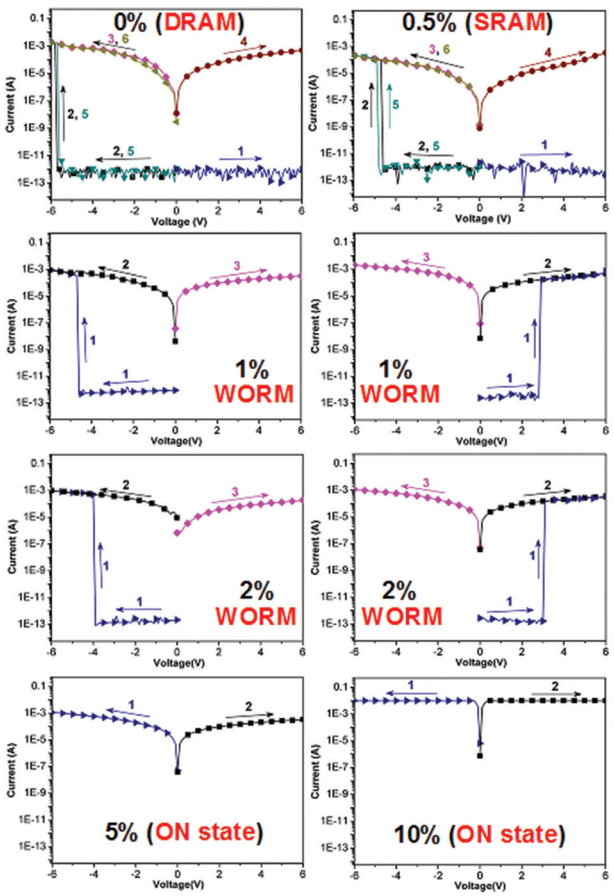

Fig. 2 Current–voltage (*I–V*) characteristics of the ITO/**OHTPA-6FPI**:PCBM/Al memory device with various PCBM weight fractions.

Fig. 2 also summarized the *I–V* results of **OHTPA-6FPI**:PCBM hybrids with various PCBM weight fractions. After incorporating 0.5 wt% of PCBM, the resulting hybrid revealed a slightly lower switching-on voltage (−4.7 V) with a SRAM characteristic. For the SRAM effect, the device could maintain the ON state after turning off the power for a longer period of time than that observed in the DRAM device (few minutes to an hour). Even with the longer retention time at the ON state for the SRAM memory device, it is also volatile and the ON state can be relaxed to the OFF state without needing an erasing process. By increasing the PCBM fraction to 1 and 2 wt%, the threshold voltage of the hybrid films gradually decreased accompanied by an increasing retention time of memory devices. The memory device could not be reset to the initial OFF state by applying a reverse electric field meaning non-erasable behavior. In addition, the ON state could also remain once the memory devices have been switched to the ON state at around 4.0–4.5 V, even after turning off power for an extended period of time (longer than a few hours).

These results demonstrate that both the hybrid films exhibit nonvolatile WORM memory properties, a permanent storage of information even after turning off power for hours. The mechanism associated with the memory characteristics was proposed by the charge transfer from the TPA donor to the PCBM acceptor, which stabilized the charge separation state and retained the high conductance state for a long time at the ON stage. Furthermore, we found that devices with 5 or 10 wt% of PCBM intrinsically exhibited high conductivity in positive/negative voltage sweeps, which could be attributed to some larger PCBM aggregates formation and bridge two electrodes, thus resulting in a conductive state.

On the other hand, the *I–V* results of polyamides **OHTPA-PA** and **OHTPA-6FPA** shown in Fig. S6 and S7† indicate insulator and SRAM memory behaviors, respectively. The insulator characteristic of the **OHTPA-PA**-based memory device can be ascribed to a weak donor–acceptor capability within the polymer chains. On the other hand, the longer retention time for **OHTPA-6FPA** as opposed to **OHTPA-6FPI** could be ascribed to the conformation effect and higher dipole moment. The conformation of the benzamide unit in **OHTPA-6FPA** is not a planar structure, which may hinder the back CT occurring; besides, higher dipole moment also facilitates and stabilizes

Table 1 Summarized memory properties of hybrid materials

	PCBM blending amounts (wt%)					
Code	0	0.5	1.0	2.0	5.0	10.0
OHTPA-6FPI	DRAM	SRAM	WORM	WORM	Conductor	Conductor
OHTPA-PA	Insulator	DRAM	WORM	WORM	Conductor	Conductor
OHTPA-6FPA	SRAM	WORM	WORM	WORM	Conductor	Conductor

the CT complex, resulting in a longer retention time for the polyamide system after removing applied power.

Moreover, Fig. S6 and S7† also depict the *I–V* results of **OHTPA-PA**:PCBM and **OHTPA-6FPA**:PCBM hybrids with various PCBM fractions, respectively. Similarly, the retention time of these memory devices exhibited an increased tendency when increasing the PCBM fractions. For **OHTPA-PA**:PCBM hybrid materials, the memory behavior changed from insulator through DRAM to WORM; meanwhile, the memory devices based on **OHTPA-6FPA**:PCBM also revealed tunable memory characteristics from SRAM to WORM. The memory properties of these high-performance polymers and their hybrid films are summarized in Table 1. These results confirm that the polymeric memory properties could be effectively manipulated through the incorporation of various amounts of the electron-acceptor PCBM.

Moreover, the effect of an operation time on the ON and OFF states of the ITO/polymer-PCBM/Al device with continuous −1 V was investigated as shown in Fig. S8,† and no obvious degradation in the current could be observed at both ON and OFF states for at least 1 hour in the readout test, revealing the excellent stability of the device.

Morphology analyses

The morphology of **OHTPA-6FPI**/PCBM hybrid films was further analyzed by TEM measurement as shown in Fig. S8.† The dark regions indicate the formation of PCBM clusters, which are well dispersed in the matrix **OHTPA-6FPI**, and the diameter becomes larger with increasing the weight fraction of PCBM. The higher amount of PCBM clusters dispersed well within the matrix **OHTPA-6FPI** could stabilize the charge separation state and inhibit the back charge recombination even under the reverse bias. Thus, the ON state can be retained for a longer time by increasing the PCBM amount and fine-tune the memory devices from DRAM through SRAM to WORM type memory characteristics.

Switching mechanism

To get more insight into the switching mechanism, molecular simulation on the basic unit was carried out by DFT/B3LYP/6-31G(d) with the Gaussian 09 program. The charge density isosurfaces of the basic unit and the most energetically favorable geometry are summarized in Fig. 3. For all the polymers, the HOMO energy levels were mainly at the electron-donating OHTPA moieties, while the LUMO energy levels were located at the electron-withdrawing phthalimide or benzamide units.

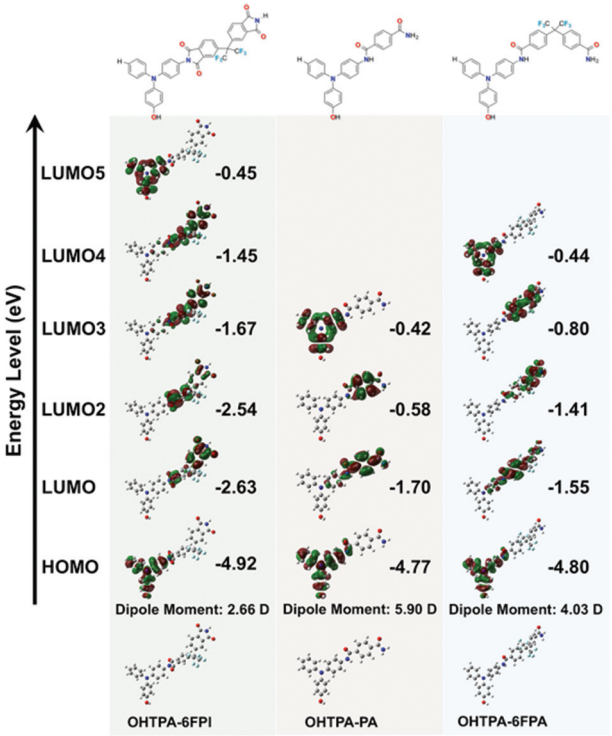

Fig. 3 Calculated molecular orbitals and corresponding energy levels of the basic units for OHTPA-based polymers.

Accordingly, the high external applied electric potential may facilitate electron transfer from the HOMO of the donor OHTPA moiety to the LUMO of the acceptor (phthalimide, benzamide, or PCBM in the hybrid system) due to the charge transfer mechanism.[4a] In the hybrid system, the partially filled LUMO and HOMO of PCBM and TPA moieties resulted in negative and positive charges, respectively. Therefore, carriers can be generated within the polymer hybrid for bringing out a tremendous decrease in electric resistance and an abrupt increase in the conductivity after charge transfer.

The solid state photoluminescence (PL) spectra of **OHTPA-6FPI** and **OHTPA-6FPI**:PCBM hybrid materials are as presented in Fig. S9.† In comparison with pristine **OHTPA-6FPI**, the fluorescence intensity of **OHTPA-6FPI**:PCBM hybrids was obviously quenched more than 40% as the PCBM fraction increased up to 10 wt%, indicating the charge transfer from the electron-donating OHTPA within **OHTPA-6FPI** to the well-dispersed electron-accepting PCBM. Thus, the charge transfer

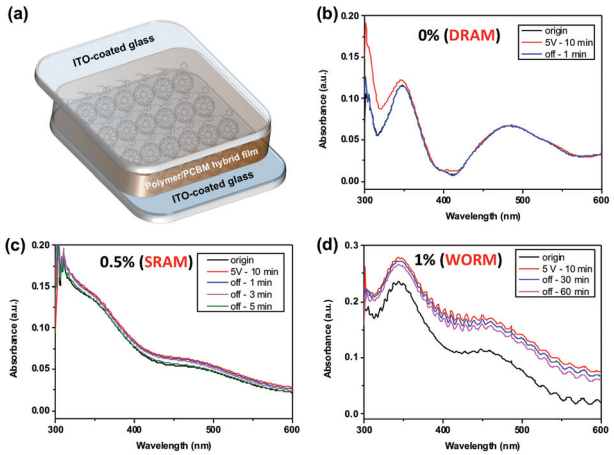

Fig. 4 *In situ* UV-visible spectra of the polymer memory devices of ITO/**OHTPA-6FPI**:PCBM/ITO during switch-ON: (a) the transparent device configuration, (b) 0% PCBM, (c) 0.5% PCBM, and (d) 1.0% PCBM.

phenomenon could occur once the applied voltage overcomes the energy barrier, then the generated carriers and charged moieties consequently induce a sharp increase in the current.

Furthermore, "*in situ*" UV-vis absorption spectroscopy during the switching-ON of **OHTPA-6FPI** and its hybrid materials was utilized as direct evidence for field induced charge transfer memory behavior, and was carried out using transparent memory devices as shown in Fig. 4a. Fig. 4b depicts the UV-vis spectra of the memory device with 0 wt% of PCBM before and after switching to the ON state, and the absorption changes after turning off the power. By switching the device from the OFF to the ON state, the intensity of the absorption peak at around 350 nm gradually increased, while this peak decreased in intensity after turning off the power and then recovered to the original state for only 1 minute. This short retention time of the UV-vis absorption change after turning off the power was similar to the DRAM behavior. Compared to 0 wt% of PCBM, the absorption peak of 0.5 wt% of PCBM slowly decreased in intensity, and could also recover the original OFF state after turning off the device for 5 minutes, as shown in Fig. 4c. The same measurement of **OHTPA-6FPI** with 1.0 wt% of PCBM is shown in Fig. 4d, but the absorption peak did not return to the original absorption OFF state even after turning off the device for 60 minutes. These "*in situ*" UV-vis absorption spectra measurements provide direct and solid evidence for the formation of the charge transfer complex, and make the field induced charge transfer theory an acceptable mechanism.

Conclusions

Three series of high ON/OFF ratio ($\sim 10^9$) memory devices were prepared based on OHTPA-based high-performance polymers with various amounts of electron-acceptor PCBM. Memory devices based on the high-performance polymers, **OHTPA-6FPI**, **OHTPA-PA**, and **OHTPA-6FPA**, exhibited DRAM, insulator, and SRAM memory properties, respectively. By introducing different PCBM fractions into OHTPA-based polymers, the memory behavior of these devices can be controlled in a wide range from insulator through DRAM, SRAM to WORM. These results demonstrate that the polymer memory characteristics can be effectively manipulated through the structural design of the electron-donating matrix and the incorporation of the electron-acceptor PCBM.

Acknowledgements

The authors grateful acknowledge the Ministry of Science and Technology of Taiwan for the financial support, and also C.-W. Lu and S.-L. Huang in the Instrumentation Center of the National Taiwan University for CHNS elemental analysis (EA) and Nuclear magnetic resonance (NMR) experiments, respectively.

Notes and references

1 (*a*) L. J. Huo, J. H. Hou, S. Q. Zhang, H. Y. Chen and Y. Yang, *Angew. Chem., Int. Ed.*, 2010, **49**, 1500; (*b*) D. Lee, E. Hubijar, G. J. D. Kalaw and J. P. Ferraris, *Chem. Mater.*, 2012, **24**, 2534.

2 (*a*) Q. B. Pei, G. Yu, C. Zhang, Y. Yang and A. J. Heeger, *Science*, 1995, **269**, 1086; (*b*) R. H. Friend, R. W. Gymer, A. B. Holmes, J. H. Burroughes, R. N. Marks, C. Taliani, D. D. C. Bradley, D. A. Dos Santos, J. L. Bredas, M. Logdlund and W. R. Salaneck, *Nature*, 1999, **397**, 121.

3 (*a*) J. Rivnay, L. H. Jimison, J. E. Northrup, M. F. Toney, R. Noriega, S. F. Lu, T. J. Marks, A. Facchetti and A. Salleo, *Nat. Mater.*, 2009, **8**, 952; (*b*) H. Yan, Z. H. Chen, Y. Zheng, C. Newman, J. R. Quinn, F. Dotz, M. Kastler and A. Facchetti, *Nature*, 2009, **457**, 679.

4 (*a*) Q. D. Ling, D. J. Liaw, C. X. Zhu, D. S. H. Chan, E. T. Kang and K. G. Neoh, *Prog. Polym. Sci.*, 2008, **33**, 917; (*b*) S. J. Liu, P. Wang, Q. Zhao, H. Y. Yang, J. Wong, H. B. Sun, X. C. Dong, W. P. Lin and W. Huang, *Adv. Mater.*, 2012, **24**, 2901; (*c*) S.-J. Liu, Z.-H. Lin, Q. Zhao, Y. Ma, H.-F. Shi, M.-D. Yi, Q.-D. Ling, Q.-L. Fan, C.-X. Zhu, E.-T. Kang and W. Huang, *Adv. Funct. Mater.*, 2011, **21**, 979; (*d*) W.-P. Lin, S.-J. Liu, T. Gong, Q. Zhao and W. Huang, *Adv. Mater.*, 2014, **26**, 570.

5 (*a*) H. J. Yen and G. S. Liou, *Polym. Chem.*, 2012, **3**, 255; (*b*) H.-J. Yen, C.-J. Chen and G.-S. Liou, *Adv. Funct. Mater.*, 2013, **23**, 5307.

6 A. Stikeman, *Technol. Rev.*, 2002, **105**, 31.

7 S. Moller, C. Perlov, W. Jackson, C. Taussig and S. R. Forrest, *Nature*, 2003, **426**, 166.

8 T. W. Kim, D. F. Zeigler, O. Acton, H. L. Yip, H. Ma and A. K. Y. Jen, *Adv. Mater.*, 2012, **24**, 828.

9 H. C. Wu, A. D. Yu, W. Y. Lee, C. L. Liu and W. C. Chen, *Chem. Commun.*, 2012, **48**, 9135.

10 (*a*) X. D. Zhuang, Y. Chen, G. Liu, P. P. Li, C. X. Zhu, E. T. Kang, K. G. Neoh, B. Zhang, J. H. Zhu and Y. X. Li, *Adv. Mater.*, 2010, **22**, 1731; (*b*) Y.-C. Lai, K. Ohshimizu, W.-Y. Lee, J.-C. Hsu, T. Higashihara, M. Ueda and W.-C. Chen, *J. Mater. Chem.*, 2011, **21**, 14502; (*c*) J.-C. Hsu, C.-L. Liu, W.-C. Chen, K. Sugiyama and A. Hirao, *Macromol. Rapid Commun.*, 2011, **32**, 528.

11 G. Liu, Q.-D. Ling, E. Y. H. Teo, C.-X. Zhu, D. S.-H. Chan, K.-G. Neoh and E.-T. Kang, *ACS Nano*, 2009, **3**, 1929.

12 A.-D. Yu, C.-L. Liu and W.-C. Chen, *Chem. Commun.*, 2012, **48**, 383.

13 (*a*) C.-J. Chen, Y.-C. Hu and G.-S. Liou, *Chem. Commun.*, 2013, **49**, 2804; (*b*) J. Liu, Z. Yin, X. Cao, F. Zhao, A. Lin, L. Xie, Q. Fan, F. Boey, H. Zhang and W. Huang, *ACS Nano*, 2010, **4**, 3987.

14 Y. Shirota, *J. Mater. Chem.*, 2005, **15**, 75.

15 D. M. Kim, S. Park, T. J. Lee, S. G. Hahm, K. Kim, J. C. Kim, W. Kwon and M. Ree, *Langmuir*, 2009, **25**, 11713.